受入
86-12-18
高工研図書室

EUROPEAN ORGANIZATION FOR NEUCLAR RESEARCH

CERN-EP/85-191
November 21st, 1985

ARE THERE "PROMPT" LIKE-SIGN DIMUONS?

H. Burkhardt, F. Dydak, J.G.H. DeGroot, R. Hagelberg , M. Krasny, J. May, H.J. Meyer, P. Palazzi, F. Ranjard, J. Rothberg, D. Schlatter, J. Steinberger, H. Taureg, H. Wahl and J. Wotschack.

CERN, Geneva, Switzerland.

H. Blümer, H. Brummel, P. Buchholz, J. Duda, F. Eisele, B. Kampschulte, K. Kleinknecht, J. Knobloch, E. Müller, B. Pszola, B. Renk and K. Schmitz.

Institut für Physik der Universität, Dortmund, Fed. Rep. Germany.

R. Belusevic, B. Falkenburg, T. Flottmann, R. Geiges, C. Geweniger, V. Hepp, H. Keilwerth and K. Tittel.

Institut für Hochenenergiephysik der Universität, Heidelberg, Fed. Rep. Germany.

P. Debu, C. Guyot, S. Loucatos, J.P. Merlo, A. Para, P. Perez, F. Perrier, B. Peyaud, J. Rander, J.P. Schuller, R. Turlay and B. Vallage.

DPhPE, CEN - Saclay, France

H. Abramowicz and J. Krolikowski.

Institute of Experimental Physics, University of Warsaw, Poland.

J.T. He, T.Z. Ruan and W.M. Wu.

Institute of High Energy Physics, Academia Sinica, Beijing, The People's Republic of China.

(Submitted to Zeitschrift f. Physik)

1. ABSTRACT

From exposures of the CDHS detector at the CERN SPS we have obtained 367 $\mu^-\mu^-$ events in neutrino beams and 73 $\mu^+\mu^+$ events in an antineutrino beam. The magnitude of a prompt like−sign signal has been controversial in the past and moreover could not be explained by known production mechanisms. A critical discussion of the experimental situation is given. We have tried to reduce the systematic uncertainties of previous experiments and to get more information on the dependence of the signal with energy and the muon momentum cut−off. This experiment yields a signal of 2.8σ (2.4σ) of prompt like−sign dimuon events in the case of neutrinos (antineutrinos). The rate to charged current events is of the order of 10^{-4} for $p_\mu > 9$ GeV and $E > 100$ GeV. The prompt signal has all the properties expected from the production and decay of charm−anticharm events. The magnitude, however, is substantially higher then the prediction of perturbative QCD but lower than some other experiments.

1. INTRODUCTION

Both the experimental situation and the theoretical interpretation of neutrino produced like−sign dimuons are still far from clear. We begin here with a brief review of the experimental situation. The earliest experiments [1−3] gave indications for, but did not convincingly demonstrate, the existence of prompt like−sign dimuons. Although of the order of fifty events had been seen in the two latter experiments [2,3], the backgrounds, chiefly from pion and kaon decay, were estimated to be of the same order of magnitude and somewhat uncertain. The CDHS experiment [2] did have the power to give useful upper limits on the "wrong sign" like−sign dimuon reactions $\nu + N \to \mu^+ + \mu^+ + X$ and $\bar{\nu} + N \to \mu^- + \mu^- + X$, because the exposures were in narrow band beams, with little antineutrino contamination in the neutrino beam and vice versa.

These early experiments were followed in 1979 by a second CDHS publication [4] based on considerably higher statistics. Two hundred and ninety examples of the reaction $\nu + N \to \mu^- + \mu^- + X$ and 53 of the reaction $\bar{\nu} + N \to \mu^+ + \mu^+ + X$ yielded, after background subtraction, the respective prompt signals 67 ± 37 and 19 ± 10. Despite the increase in statistics, the significance of the signal was still less than two standard deviations in either case.

In 1981 three groups published new results, the HPWF [5], the CCFRR [6], and the CHARM [7] Collaborations. The CCFRR results have since been revised [8]. In Fig. 1 all previous results for the ratio of like−sign to single−muon cross−sections are shown as a function of the total measured energy, E_{vis}. The experimental points, in general, increase steeply with energy and are not, on the whole, in disagreement with each other, given the large quoted errors. However, the CDHS point is quite low with respect especially to the CHARM results [7].

Comparison with bubble−chamber publications [9] on the closely related neutrino production of like−sign muon−electron pairs, in the hope of resolving this contradiction, is difficult because the energy cut−off for the electrons is usually less than 1 GeV in these experiments, and above 6 GeV no results are available.

Theoretically, the only possible source for like sign dimuons, if we restrict ourselves to known particles and interactions, is the creation of a charm – anticharm pair in the hadron shower of a normal charged – current interaction. But perturbative QCD calculations [10] lead to rates which are considerably lower than those experimentally reported. Although it is possible to imagine non – perturbative contributions which are much bigger [11], quantitative calculations are not possible in the present state of the theory, and in the somewhat parallel intermediate photon production of charmed quark pairs, observed in dimuon production by muons, perturbative QCD seems successful [12, 13].

Given the experimental questions referred to above, and the importance of the result, since new physics may be indicated, we have decided to attack the problem once again. Our main concern in this new effort was an improvement in the systematics of the background subtractions. To this end, as was not the case in our previous work, the reconstruction and selection of the events is done by the computer without human intervention[1].

2. NEUTRINO BEAMS AND DETECTOR

The results presented here were obtained in the CDHS detector exposed to three different neutrino beams at the CERN 450 GeV Super Proton Synchrotron:

1. A 300 GeV narrow band beam (NBB) neutrino exposure in 1979/80. In this beam secondary hadrons are momentum selected to 300 GeV ± 5% and focused to a parallel beam (divergence ~ 0.2 mrad) for the traversal of the 300 m long decay tunnel. This beam has the disadvantage of limited intensity, but the advantage that the antineutrino background is very low. The integral proton intensity on target was 2.2×10^{18}.

---

[1] Previously we have analysed a data sample of similar size [14]. At the time data were selected and reconstructed by human interaction which did not allow a reliable calculation of the systematic uncertainty. However, the result of the former work is in agreement with the result of this analysis which is superior from the point of view of systematics.

2. A 400 GeV wide band beam (WBB) neutrino exposure in 1983. In this beam 400 GeV protons strike a target. The positive hadrons emitted in the forward directions are achromatically focused in a Van der Meer horn [15], and the negative hadrons defocused. The integral proton intensity was 1.3 x 10^{18}.
3. A 400 GeV WBB antineutrino beam, produced in the same horn with reversed current. The integral proton intensity was 2.6 x 10^{18}.

The yields of the inclusive charged−current process, $\nu(\bar{\nu})$ + Fe → $\mu-(\mu+)$ + X for the three exposures are shown in Fig. 2 as a function of the energy of the neutrino events. Since the cross−section of the charged−current reaction is proportional to the neutrino energy, the neutrino and antineutrino spectra can be read from Fig. 2.

The detector used in the ν NBB exposure has been described previously [16]. Briefly, it consists of 19 modules of 3.75 m diameter iron plates, toroidally magnetized. Each module has a total iron thickness of 75 cm and a mass of ~ 70 t. Scintillator planes between iron plates are used to measure the energy of the hadronic shower. Drift chambers between modules, each in three projections, measure the muon trajectory. The detector has three important advantages with respect to other detectors, especially for the study of like−sign dimuons:

1. The geometrical acceptance for both muons is very near unity, since both are focused towards the detector axis.
2. The mean free path for hadronic decay is short, since the density is high. This is important since the basic problem is the detection of a prompt signal above hadron decay background.
3. The fiducial mass is large. This is important because the like−sign rates are low.

Between the NBB run and the later WBB runs in 1983 the detector was improved. Eight of the modules were replaced by ten new modules. The latter were thinner, containing only 50 cm of iron plate in place of 75 cm, and the sampling thickness decreased from 5 cm to 2.5 cm of iron. Furthermore, the scintillator strips were narrower, and, alternately, in both vertical and horizontal projection, so that the spatial reconstruction of the hadron shower was improved. These modifications were only of secondary importance in the study of like−sign dimuons.

Events were accepted if:

1. The vertex was inside a radius of 1.6 m. A small rectangular region at the centre of the modules where the magnetization coil passes, 0.3 x 0.2 m for the old and 0.1 x 0.1 m for the new modules, was excluded.
2. In the NBB exposure the vertex was required to be within the iron thickness 0.15 – 9.75 m, leaving a minimum of six modules for muon momentum measurement at the end of the detector. For the WBB exposures the vertex was required to be within the iron thickness 0.25 – 8.75 m, leaving a minimum of six modules. The corresponding fiducial masses were 650 t and 540 t, respectively.
3. Both tracks were required to traverse at least six drift chambers to assure an acceptable reconstruction efficiency.
4. The first track has to start at least in the third drift chamber downstream from the vertex.
5. The distance between the two–muon tracks as projected on the vertex plane is smaller than 20 cm.

A typical like–sign event is shown in Fig. 3.

In order to make comparison possible with the charged–current rates, as well as to permit the calculation of the pion and kaon decay background, single–muon events were also recorded, but at the reduced, scaled rate of 1 in 64.

The calculated geometrical acceptances for the three inclusive reactions, single–muon (charged–current), opposite–sign dimuon and like–sign dimuon, are shown in Table 1.

3. EXPERIMENTAL RESULTS

Events were computer selected and reconstructed. In addition to like−sign dimuon events, charged−current and opposite−sign dimuon events were also retained in order to make rate comparisons possible. From the measured muon energies, E_1 and E_2, and the hadron shower energy E_H we calculate the visible energy $E_{vis} = E_1 + E_2 + E_H$ of the event. The data were divided into three bins of visible energy : 30 − 100 GeV, 100 − 200 GeV and 200 − 300 GeV, and tabulated for three minimal values of the muon momentum: $p_\mu > 6$ GeV, $p_\mu > 9$ GeV, and $p_\mu > 15$ GeV. For dimuon events the measured energy E_{vis} is not, even apart from experimental resolution effects, the true neutrino energy, since in general a neutrino is missing. In the case of opposite−sign dimuons this average missing energy is ~ 12%. The raw event numbers are given in Table 2. We point out that the luminosity (neutrino flux x fiducial mass x dimuon detection efficiency) of this experiment is about five times that of the nearest other experiment [7].

The raw data must be corrected for geometrical acceptance, reconstruction efficiency, and the background must be subtracted. The geometrical acceptances have been calculated by Monte Carlo technique, under assumptions for the angular and momentum distributions of the muons according to the measured structure functions in the case of single−muon events, according to the charm hypothesis in the case of opposite−sign dimuon events and according to the π/K decay Monte Carlo program in the case of like−sign dimuon events, and have been given in Table 1. The opposite−sign dimuon acceptance is smaller than the like−sign because the second muon is outbending in the magnetic field and therefore has a greater probability of leaving the detector before satisfying the range requirement of six chambers traversed.

The reconstruction efficiency was determined by scanning a fraction of the events which satisfied the two−muon trigger, independently of success or failure in the reconstruction program. These efficiencies are given in Table 3.

The background is dominated by muons produced in the decay of pions and kaons in the hadron shower, but there are also non−negligible backgrounds due to trimuon events in which one muon of the secondary pair has a momentum of less than 6 GeV, and "overlay" events in which two independent charged−current events are so close in space and time that they are not distinguished by the reconstruction program.

The π and K decay background is obtained by a Monte Carlo calculation in which charged−current hadron shower energies are generated according to the observed distributions, and the individual hadrons in each shower are generated according to both experimental and theoretical information available. It is the uncertainty in the hadron shower fragmentation which is entirely responsible for the uncertainties in this calculation, since the other parameters which enter − detector density and geometry, and pion and kaon lifetimes − are well known. As much as possible the data were taken from neutrino interactions observed in bubble chambers. Here we are grateful to our colleagues from the experiments with the 15 ft FNAL chamber with neon filling, with the CERN BEBC chamber, also filled with neon, and with BEBC, filled with deuterium, who very kindly supplied us with unpublished compilations of their fragmentation data[2]. These data are of course immensely valuable for this calculation, but suffer also from clear limitations, chiefly the sparseness of data at high energies, some disagreements between the data in details, and the lack of K^+ and K^- identification. To cope with the latter we made use of fragmentation calculations based on the Lund model[3]. We proceeded as follows. Use was made of the fact that the distribution in the variable z, the fraction of the shower energy carried by the individual hadron, is rather insensitive to shower energy in the range of interest here, except at very low z where the contribution is small because of the cut in minimum muon momentum. The shape of the pion z distributions was obtained by a fit to all bubble chamber data available to us, of the form $A\, e^{-Bz}$, $z > z_0$, and $C\, e^{-Dz}$, $z < z_0$, separately for leading and non−leading pions. The

---

[2] We wish to express our thanks to Prof. C. Baltay, Dr. A.M. Cooper, Dr. B. Nellen and Dr. R. Wigmans for their kind collaboration.

[3] We wish to express our thanks for the collaboration of Drs. D. Bertrand and R. Wigmans who performed these calculations for our conditions.

ratio of kaons to pions was also obtained from the bubble chamber data, using K^0 data, and assuming $N^{K^+} + N^{K^-} = N^{K^0} + N^{\overline{K^0}}$. The z dependences for the charged kaons were obtained by fitting exponentials to the Lund model calculations. An overall normalization was imposed to require pions and kaons to account for 95% of the shower energy, assuming $N^{\pi^0} = 1/2(N^{\pi^+} + N^{\pi^-})$ and $N^{K^0} + N^{\overline{K^0}} = N^{K^+} + N^{K^-}$. The z distributions which were finally used are given in Table 4. But many variations, based on other fits and also on unfitted data, were tried as well. On the basis of these variations, we believe that the uncertainties in the π/K decay subtraction are not more than 15%, and this error has been applied throughout.

A second, substantially smaller, background contribution to like−sign dimuon events is due to trimuon events. Trimuons in neutrino interactions have been observed by several experiments after the first observation in 1977 [17, 18]. The observed rate is only $\sim 3\times10^{-5}$ of ordinary charged−current events.

Trimuons have been quantitatively understood [18] in terms of the electromagnetic radiation of a muon pair either by the primary muon or by the hadronic shower. In the like−sign dimuon sample, trimuons are contained if the μ^+ (for neutrino) or the μ^- (for anti−neutrino) has an energy less than the 6 GeV required in our event selection, while the other two have energies above the respective momentum cuts (6, 9 or 15 GeV). To estimate that background, we have used calculations due to J. Smith and G. Valenzuela[4] [19] which give a good description of our old trimuon data [18]. The overall amount of this background is about 8% of the raw dimuon sample.

In order to understand the overlay background, a large number of overlay events were generated by combining into one event two successive normal, independent charged− current events. The two superposed events were of course in time with their respective trigger. The effect of the time delay in the second of the two events falsifies the energy measurement and produces an inefficiency in the scintillator signals if the delay exceeds 100−200 ns. This time delay also invalidates the drift time measurement in such a way that the reconstruction efficiency for delayed muons is largely reduced. These

[4] We thank Prof. J. Smith and Dr. G. Valenzuela for providing us with calculations which take proper account of the neutrino spectra and data selection cuts of this experiment.

effects were measured and then the second event in the artificially created overlays was modified accordingly.

The final quantitative understanding of the overlay background is based on a study of the distribution in Δr, the distance between the two−muon tracks as projected back to the vertex plane, for "true" events and artificial overlays (Fig. 4). The true events have a peak at small Δr due to genuine dimuon events and a tail at large Δr due to overlays. The artificial overlay events reproduce this tail exactly, but go to zero at small r. The event selection cut was $\Delta r < 20$ cm. The two curves were normalized for $r > 40$ cm. The rates and kinematic distributions of the so normalized artificial overlays for $\Delta r < 20$ cm were used in the determination of this background. It is in general quite small, but in the region of large p_μ and large transverse muon momentum, $p_{T\mu}$, it becomes quite important, since such events, though rare, could be of great interest. The systematic uncertainty in this subtraction is estimated at 30% and included in the evaluation of the prompt signal uncertainty.

The importance of the background subtractions can be seen in Fig. 5. They are very severe at low neutrino energy where the neutrino flux is high and where most events are found, and relatively lower, but still appreciable, at higher neutrino energy. The severity of the background also decreases with increasing muon momentum cut−off, so that in our data the most convincing positive results for the existence of like−sign dimuons are found for $p_\mu > 9$ GeV. They are, for neutrinos, with $p_\mu > 9$ GeV and $100 < E_{vis} < 300$ GeV:

$$\frac{\sigma \text{ like}-\text{sign}}{\sigma \text{ charged}-\text{current}} = \frac{\mu^-\mu^-}{\mu^-} = (1.16 \pm 0.42) \times 10^{-4}$$

and

$$\frac{\sigma \text{ like}-\text{sign}}{\sigma \text{ opp.}-\text{sign}} = \frac{\mu^-\mu^-}{\mu^-\mu^+} = (3.2 \pm 1.2) \times 10^{-2},$$

2.8 standard deviations above zero, and for antineutrinos, with $p_\mu > 9$ GeV and $100 < E_{vis} < 300$ GeV :

$$\frac{\sigma \text{ like-sign}}{\sigma \text{ charged-current}} = \frac{\mu^+\mu^+}{\mu^+} = (1.7 \pm 0.7) \times 10^{-4}$$

and

$$\frac{\sigma \text{ like-sign}}{\sigma \text{ opp.-sign}} = \frac{\mu^+\mu^+}{\mu^+\mu^-} = (5.1 \pm 2.3) \times 10^{-2},$$

2.4 standard deviations from zero.

The complete prompt results for the three muon momentum cuts and the three energy bins are given in Table 5. The dependence on the visible energy is shown in Fig. 6 for $\sigma_{like-sign}/\sigma_{charged-current}$ and in Fig. 7 for $\sigma_{like-sign}/\sigma_{opp-sign}$. The dependence on the minimum muon momentum is shown in Fig. 8.

To illustrate some properties of the prompt like-sign dimuon data we show in Figs. 9 to 13 distributions of various physics quantities for neutrino events of the WBB exposure. The definition of the "second muon" was done by selection of the smaller transverse momentum with respect to the shower direction.

From the measured muon energies, E_1 and E_2, and the hadron shower energy E_H we calculate the visible energy $E_{vis} = E_1 + E_2 + E_H$ of the event and the scaling variable $y_{vis} = (E_H + E_2)/E_{vis}$. Using the measured angle θ_1 of the leading muon relative to the neutrino direction, we obtain $x_{vis} = 2 E_1 E_{vis} \sin^2(\theta_1/2)/[(E_2 + E_H)M_p]$.

4. DISCUSSION OF RESULTS

The results presented in the previous section are in agreement with our published results [2,4], but more significant. They indicate a prompt like−sign signal both in neutrino and antineutrino reactions at a level of two to three standard deviations. The neutrino energy dependence is similar to that for opposite−sign dimuons [20]. Since the opposite−sign energy dependence is due to a threshold effect, namely the production of a charmed quark, a similar basis for the like−sign dimuon signal energy dependence is indicated. Other kinematic properties (see Figs. 9 to 13) make it quite clear that the extra muon is associated with the hadronic shower, and is therefore the decay product of a hadron which cannot have a mass appreciably larger than that of charm, because the observed transverse momenta with respect to the shower are small. This excludes a separation of π/K background and the prompt signal using kinematic properties. Events at large transverse momenta are consistent with being background, mostly overlays of two charged−current events. We observe seven events with $p_{T\mu} > 2$ GeV where we expect six from the background (including four overlay events).

In the absence of another particle in this mass range, we believe that the origin of these events can only be the production and decay of charm. This charm production is of course totally different from the production of charm via the flavour changing current, which results only in opposite−sign dimuons and in this case is well understood. Like−sign dimuons require, in the standard model, the production of a charm−anticharm pair in the final−state hadronic system. This production has been estimated on the basis of conventional first−order QCD models [21]. We have used the very detailed work of Hagiwara [10] for the QCD cross−section. This model has uncertainties of up to a factor of 3 due to the strong dependence on the quark mass and due to possible intermediate production of the J/Ψ. This calculation, however, integrates over the entire muon spectrum, and we have estimated the effect on these calculations of our cuts on muon momentum, using a program of G. Ingelman[5], which simulates the fragmentation and decay of the charmed quark. The theoretical QCD curves shown in Figs. 6 and 8 are the results of this work. It can be seen that theory and experiment are still far apart,

[5] We wish to express our thanks to Dr. G. Ingelman for making these available to us.

the theoretical expectations are lower than our results by the factor of ~ 30.

Non−perturbative effects could, in principle, be responsible for a strong enhancement [11]. But this would be in contrast to the much better agreement of perturbative QCD of charm production in muon nucleon scattering [13]. We are not competent to resolve this difficulty. However, we want to emphasize that all other characteristics of our prompt like−sign dimuon data can be understood in terms of charm−anticharm production.

5. COMPARISION WITH OTHER EXPERIMENTS

In Fig. 14 we have plotted the ratio of neutrino−induced like−sign events to charged−current events as a function of the visible energy, together with the results of other counter experiments. The fact that our results were lower than that of the CHARM experiment [7] is still true even at higher energies. But also with respect to the HPWF result for $E_{vis} > 100$ GeV we observe less prompt events. In order to make a comparison between the results from these different experiments more meaningful, we believe some comments on the HPWF experiment [5] and the CHARM experiment [7] are useful. The disagreements are probably to be ascribed largely to differences in the background subtraction. If the background is underestimated, not only is the signal increased, but in the same measure the apparent statistical significance of the signal is also increased. The dominant background is that due to pion and kaon decay. This background is proportional to the hadron absorption mean free path in the material of the detector. In the CDHS experiment this was 29 cm, in the CCFRR experiment about the same, in the HPWF experiment it was 64 cm for the weighted average of the three detector pieces of different density, and for the CHARM experiment about 80 cm. To the extent to which the raw signal is dominated by π/K decay background, the CHARM and HPWF experiments with lower density have a correspondingly higher background. If in the publication of the 1979 results [2] the CDHS Collaboration was correct in evaluating this background at a level of 71% of the

raw signal, the corresponding figures for HPWF and CHARM would be 89% and 91%, respectively! The subtractions which were performed in these experiments were however much smaller, and this is the origin of the differences in the reported prompt like−sign rates.

In the CHARM experiment the background subtraction was performed differently. In that experiment the background is subtracted on the basis of the differences between prompt and π/K background events, in the separation between the two muons as projected back to the vertex plane through the hadron shower from the measurements of the tracks further on. If the second muon is due to the decay of a primary pion or kaon, the distribution in this separation does not differ markedly from that of the prompt dimuons, since the effect of the decay angle is obscured by the multiple scattering and measurement errors in the back projection. However, the muons due to the decay of secondary hadrons exhibit a tail at large separations. In the method employed for the evaluation of this background, the primary background was grossly underestimated because the relative attenuation of primary to secondary hadrons, before leaving the obscuration of the hadron shower, was ignored. According to our estimate, the error is sufficient to create the reported signal in the absence of any real signal. A less serious source of error in this method is that the sign of the electric charge is not measured, but the like−sign background depends very much on the charges of the more energetic hadrons (leading particle effect). Yet another puzzling feature of the publication [7] is the discrepancy in the errors between the two presentations of the like−sign signal. In the text the signal is given as $N(\mu^-\mu^-)/N(\mu^-\mu^+)\varepsilon = 0.14 \pm 0.05$ or 2.8 standard deviations, whereas in their Fig. 4 the signal is divided into two bins of E_{vis}. The errors shown (and reproduced in Fig. 1 of this paper) correspond to 3 and 5.5 standard deviations for the E_{vis} bins 20−100 and 100−200 GeV, respectively . It is our understanding that the large and significant rate of the CHARM experiment is due to the underestimation of π/K decay background.

According to our data and analysis − see Fig. 5 − the signal−to−noise ratio improves with neutrino energy and muon momentum. In this case, the experiments at the higher energies now available at FNAL may be in a good position to remove the remaining doubts about the existence of prompt like−sign dimuons.

REFERENCES:

1. A. Benvenuti et al, Phys Rev. Lett 35 (1975) 1202.
2. M. Holder et al., Phys Lett. 70B (1977) 396.
3. A. Benvenuti et al., Phys. Rev. Lett. 41 (1978) 725.
4. J.G.H. DeGroot et al., Phys. Lett. 86B (1979) 103.
5. T. Trinko et al., Phys. Rev. D23 (1981) 1889.
6. K. Nishikawa et al., Phys. Rev. Lett. 46 (1981) 1555.
7. M. Jonker et al., Phys Lett. 107B (1981) 241.
8. K. Nishikawa et al., Phys. Rev. Lett. 54 (1985) 1336.
9. H.C. Ballagh et al., Phys. Rev. D24 (1981) 7;
   V.V. Ammosov et al., Phys. Lett. 106B (1981) 151;
   A. Haatuft et al., Nucl. Phys. B222 (1983) 365;
   P. Marage et al., Z. Phys. C21 (1984) 307.
10. K. Hagiwara, Nucl. Phys. B173 (1980) 487.
11. R.M. Godbole and D.P. Roy, Phys. Rev. Lett. 48 (1982) 1711, Z. Phys. C22 (1984) 39;
    F.A. Choban, Z. Phys. C25 (1984) 269.
12. J.J. Aubert et al., Phys. Lett. 89B (1980) 267, 94B (1980) 96, 94B (1980) 101;
    A.R. Clark et al., Phys. Rev. Lett. 43 (1979) 187, 45 (1980) 682, 45 (1980) 686.
13. J.P. Leveille and T. Weiler, Nucl. Phys. B147 (1979) 147.
14. B. Peyaud in Proc. 1981 European Physical Society Conference on High Energy Physics, Lisbon, 1981, and
    J. Knobloch in Proc. 1981 International Conference on Neutrino Physics and Astrophysics, Maui, Hawaii, 1981, Vol. 1, p. 421.
15. S. Van der Meer, CERN 61−17 (1967).
16. M. Holder et al., Nucl. Instr. 148 (1978) 235.
17. B.C. Barish et al., Phys. Rev. Lett. 38 (1977) 577, 40 (1977) 432, 40 (1977) 498;
    A. Benvenuti et al., Phys. Rev. Lett. 38 (1977) 1110;
    M. Holder et al., Phys. Lett. 70B (1977) 393;
    J.G.H. DeGroot et al., Phys. Lett. 85B (1979) 131.
18. T. Hansl et al., Phys. Lett. 77B (1978) 114; Nucl. Phys. B142 (1978) 381.
19. J. Smith and G. Valenzuela, Phys. Rev. D28 (1983) 1071.

20. H. Abramowicz et al., Z. Phys. C15 (1982) 19.

21. H. Goldberg, Phys. Rev. Lett. 39 (1977) 1598;
B.L. Young et al., Phys. Lett. 74B (1978) 111;
V. Barger et al., Phys. Rev. D18 (1978) 2308.

Table 1

Calculated geometrical acceptances

	E_{vis} GeV	single-muon μ^-	opp.-sign $\mu^-\mu^+$	like-sign $\mu^-\mu^-(\nu)$, $\mu^+\mu^+(\bar{\nu})$
$p_\mu > 6$	30 - 100	.97	.57	.86
	100 - 200	.98	.71	.92
	200 - 300	.98	.80	.94
$p_\mu > 9$	30 - 100	.99	.75	.98
	100 - 200	.99	.83	.98
	200 - 300	1.0	.89	.99
$p_\mu > 15$	30 - 100	1.0	.90	1.0
	100 - 200	1.0	.93	1.0
	200 - 300	1.0	.96	1.0

Table 2

Observed charged-current, opposite-sign dimuon and like-sign dimuon event numbers.

a) ν NBB

	E_{vis} GeV	single-muon μ^-	opp.-sign $\mu^-\mu^+$	like-sign $\mu^-\mu^-$
p_μ > 6 GeV	30 - 100	11,171	12	1
	100 - 200	17,758	54	7
	200 - 300	14,755	62	9
p_μ > 9 GeV	30 - 100	10,751	12	0
	100 - 200	17,468	50	5
	200 - 300	14,632	60	7
p_μ >15 GeV	30 - 100	9,611	1	0
	100 - 200	16,888	34	0
	200 - 300	14,386	51	2

b) ν WBB

	E_{vis} GeV	single-muon μ^-	opp.-sign $\mu^-\mu^+$	like-sign $\mu^-\mu^-$
p_μ > 6 GeV	30 - 100	1,261,248	1408	171
	100 - 200	360,768	1207	158
	200 - 300	28,608	121	21
p_μ > 9 GeV	30 - 100	1,186,624	979	85
	100 - 200	352,960	1042	93
	200 - 300	28,544	109	13
p_μ >15 GeV	30 - 100	1,025,856	340	22
	100 - 200	338,304	693	36
	200 - 300	27,840	83	7

c) $\bar{\nu}$ WBB

	E_{vis} GeV	single-muon μ^+	opp.-sign $\mu^+\mu^-$	like-sign $\mu^+\mu^+$
p_μ > 6 GeV	30 - 100	598,656	530	48
	100 - 200	66,880	232	24
	200 - 300	1,728	10	1
p_μ > 9 GeV	30 - 100	582,144	357	15
	100 - 200	65,920	202	15
	200 - 300	1,728	9	1
p_μ >15 GeV	30 - 100	536,960	123	1
	100 - 200	64,832	123	6
	200 - 300	1,728	8	0

Table 3

Reconstruction efficiency

Process / P_μ >	Like-sign dimuons	Opp.-sign dimuons	Charged-Currents
6 GeV	.80 ± .04	.89 ± .02	.98 ± 0.01
9 GeV	.83 ± .07	.90 ± .04	.99 ± 0.01
15 GeV	.85 ± .07	.92 ± .04	.99 ± 0.01

Table 4

Distributions in z used in the pion and kaon decay background calculations. The distributions have been fitted to the form $\frac{dN}{dz} = \begin{cases} A\, e^{-Bz} & z > z_0 \\ C\, e^{-Dz} & z < z_0 \end{cases}$

The final column gives the normalization.

	A	B	C	D	z_0	$\int_0^1 z \frac{dN}{dz} dz$
For primary shower						
Leading pion	13.7	6.6	35.	17.1	.1	.326
Non leading pion	10.6	7.9	25.3	16.2	.1	.184
K^+	1.18	4.6	-	-	-	.053
K^-	.96	5.6	-	-	-	.030
For secondary shower						
Secondary pions	21.3	6.5	-	-	-	.501
Secondary kaons	7.5	4.0	-	-	-	.042

Table 5

Background corrected dimuon signals on ratios of prompt like-sign to charged-current and opposite-sign dimuon events.

a) (NBB and WBB combined)

	E_{vis} GeV	Prompt event numbers $\mu^-\mu^-$	$\mu^-\mu^+$	$\frac{\mu^-\mu^-}{\mu^-} \times 10^{-4}$	$\frac{\mu^-\mu^-}{\mu^-\mu^+} \times 10^{-2}$
$p_\mu > 6$	30 - 100	24. ± 26	1238 ± 41	.26± .28	1.3 ± 1.4
	100 - 200	46.5 ± 22	1131 ± 37	1.6 ± .74	3.5 ± 1.6
	200 - 300	13 ± 6.1	166 ± 14	3.8 ± 2.0	7.3 ± 3.4
$p_\mu > 9$	30 - 100	20.5 ± 13.5	898 ± 34	.20 ± .13	1.9 ± 1.2
	100 - 200	33 ± 13.5	1020 ± 14	1.05 ± .43	2.9 ± 1.2
	200 - 300	7 ± 4.9	158 ± 13	2.1 ± 1.5	4.2 ± 3.0
$p_\mu >15$	30 - 100	7 ± 5.2	317 ± 20	.08 ± .06	2.1 ± 1.6
	100 - 200	16 ± 6.7	703 ± 28	.52 ± .22	2.3 ± 1.0
	200 - 300	4.5 ± 3	131 ± 12	1.3 ± .9	3.6 ± 2.4

b) $\bar{\nu}$

	E_{vis} GeV	Prompt event numbers $\mu^+\mu^+$	$\mu^+\mu^-$	$\frac{++}{+} \times 10^{-4}$	$\frac{++}{+-} \times 10^{-2}$
$p_\mu > 6$	30 - 100	13 ± 9	483 ± 24	.32 ± .22	1.9 ± 1.35
	100 - 200	11.7 ± 5.3	218 ± 15	2.2 ± 1.0	4.5 ± 2.0
	200 - 300	.6 ± 1	9.5 ± 3.2	4.5 ± 7.5	5.7 ± 6
$p_\mu > 9$	30 - 100	3 ± 4.4	336 ± 20	.06 ± .09	.7 ± 1.1
	100 - 200	9.6 ± 3.9	195 ± 15	1.7 ± .7	4.4 ± 1.8
	200 - 300	.8 ± 1	8 ± 3	5.5 ± 7	10 ± 15
$p_\mu >15$	30 - 100	-1.1 ± 1.8	108 ± 11	-.02 ± .04	1.1 ± 1.8
	100 - 200	4.5 ± 2.5	110 ± 11	.8 ± .45	4.1 ± 2.3
	200 - 300	-	8 ± 3	-	-

FIGURES

Fig. 1 – Previous results from counter experiments on the ratio of the prompt like – sign dimuon and the charged – current cross – sections.

Fig. 2 – Observed charged – current rates as a function of the measured energy for the three beams.

Fig. 3 – Typical like – sign dimuon event. This event was observed in the WBB exposure.

Fig. 4 – Distributions in Δr, the separation of the two reconstructed muons in the vertex plane, for raw like – sign dimuon events and "overlay" events. The two curves are normalized in the region $\Delta r > 40$ cm. The event acceptance criterion is $\Delta r < 20$ cm.

Fig. 5 – Histogram to show the different background subtractions for neutrino and antineutrino like – sign dimuon events in the three bins of E_{vis} and for the three minimum muon momentum cuts.

Fig. 6 – Ratio of like – sign to charged – current cross – sections in three E_{vis} energy bins. The curve is the prediction of perturbative QCD charm – anticharm production [10].

Fig. 7 – Ratio of like – sign to opposite sign cross – sections in three E_{vis} energy bins.

Fig. 8 – Ratio of like – sign to charged – current cross – sections as function of minimum muon momentum. The dashed line is for perturbative QCD of charm – anticharm production [10] (scaled by a factor of 10).

Fig. 9 – Momentum distribution of the second muon in $\nu N \rightarrow \mu - \mu - X$.

Fig. 10 – Distribution of transverse momentum of the second muon in $\nu N \rightarrow \mu - \mu - X$.

Fig. 11 – Distribution in $\Delta\Phi$, the angle between the two muons in the plane normal to the neutrino direction, for $\nu N \rightarrow \mu - \mu - X$.

Fig. 12 – Distribution in the scaling variable $y_{vis} = (E_H + E_2)/E_{vis}$ in $\nu N \rightarrow \mu - \mu - X$.

Fig. 13 – Distribution in the scaling variable $x_{vis} = 2 E_1 E_{vis} \sin^2(\theta_1/2)/((E_2 + E_H)M_p)$.

Fig. 14 – Ratio of like – sign to charged – current cross – sections in neutrino interactions as a function of visible energy.

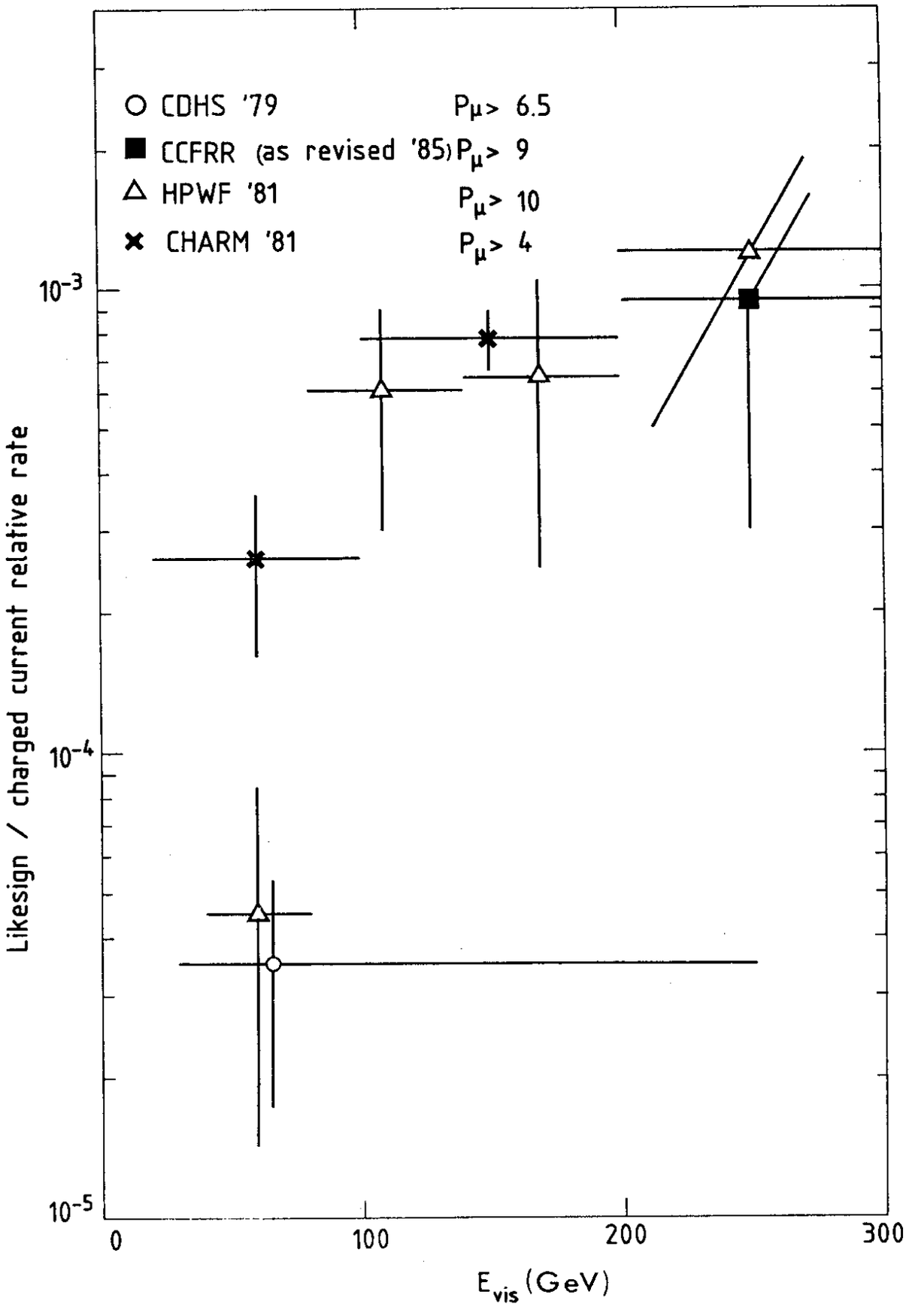
O CDHS '79 Pμ> 6.5
■ CCFRR (as revised '85) Pμ> 9
△ HPWF '81 Pμ> 10
✖ CHARM '81 Pμ> 4
10⁻³
10⁻⁴
10⁻⁵
Likesign / charged current relative rate
0
100
200
300
E_vis (GeV)

Fig. 1

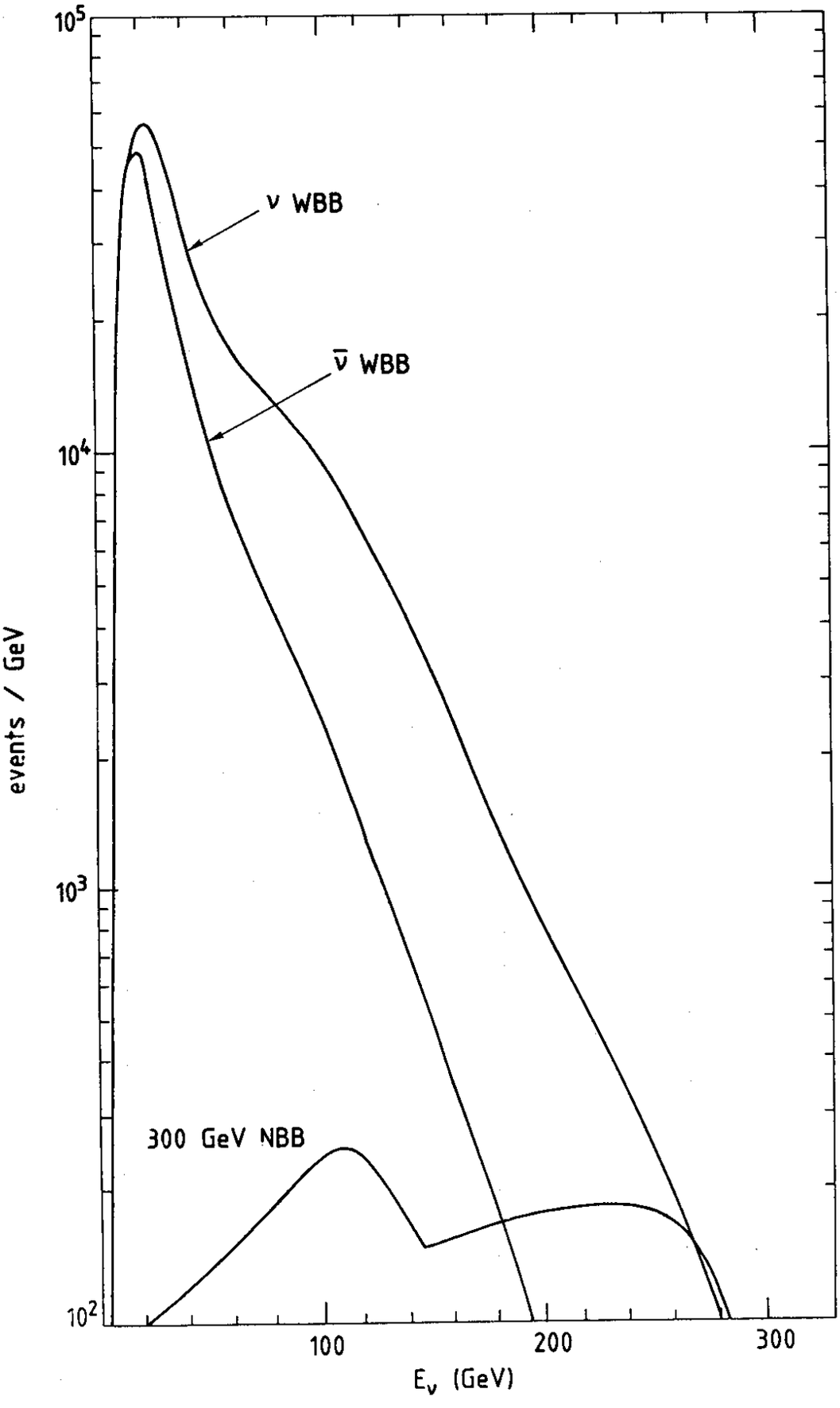
10^5
10^4
10^3
10^2
events / GeV
ν WBB
$\bar{\nu}$ WBB
300 GeV NBB
100
200
300
E_ν (GeV)

Fig. 2

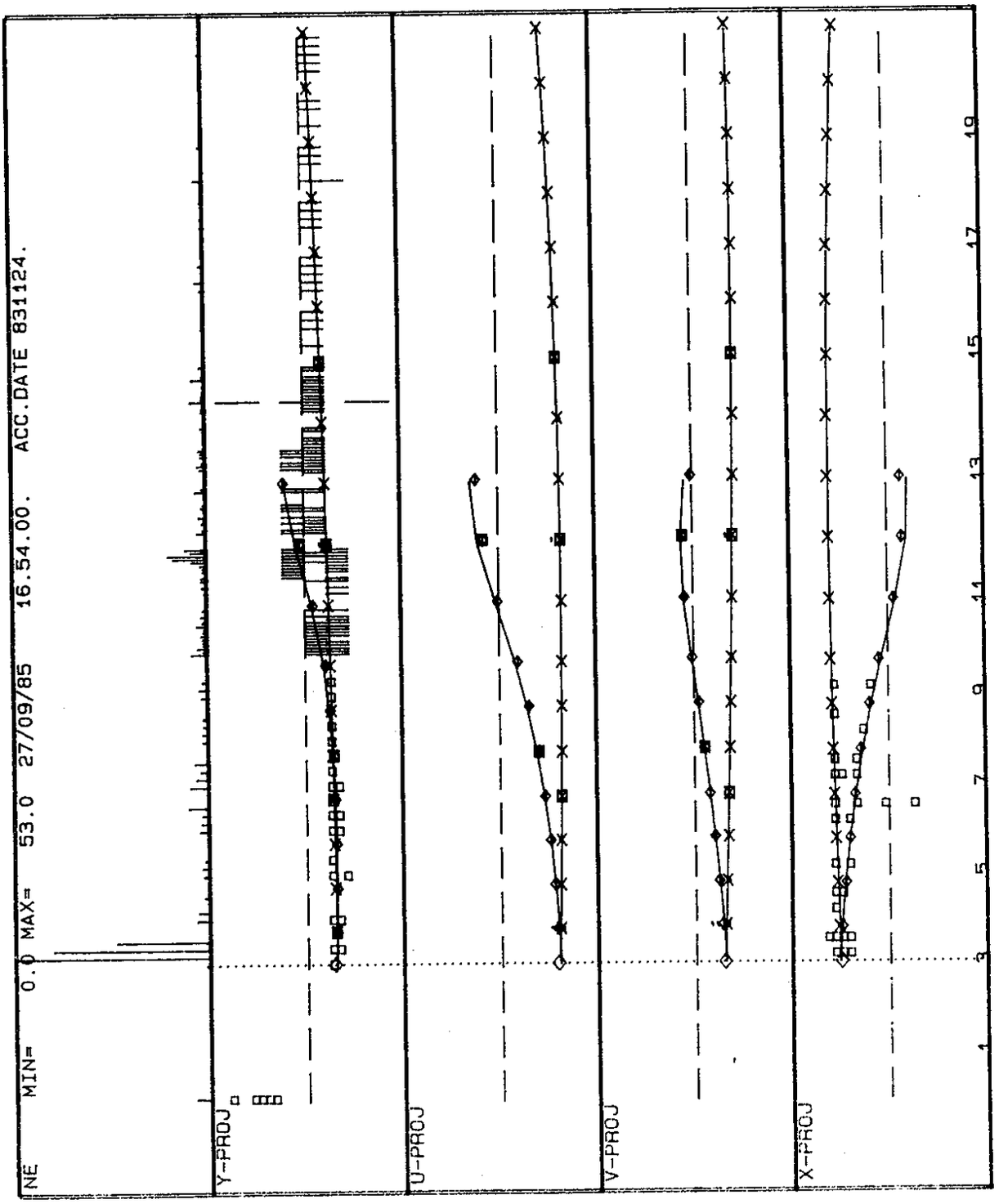
NE MIN= 0.0 MAX= 53.0 27/09/85 16.54.00. ACC.DATE 831124.
Y-PROJ
U-PROJ
V-PROJ
X-PROJ
1
3
5
7
9
11
13
15
17
19

Fig. 3

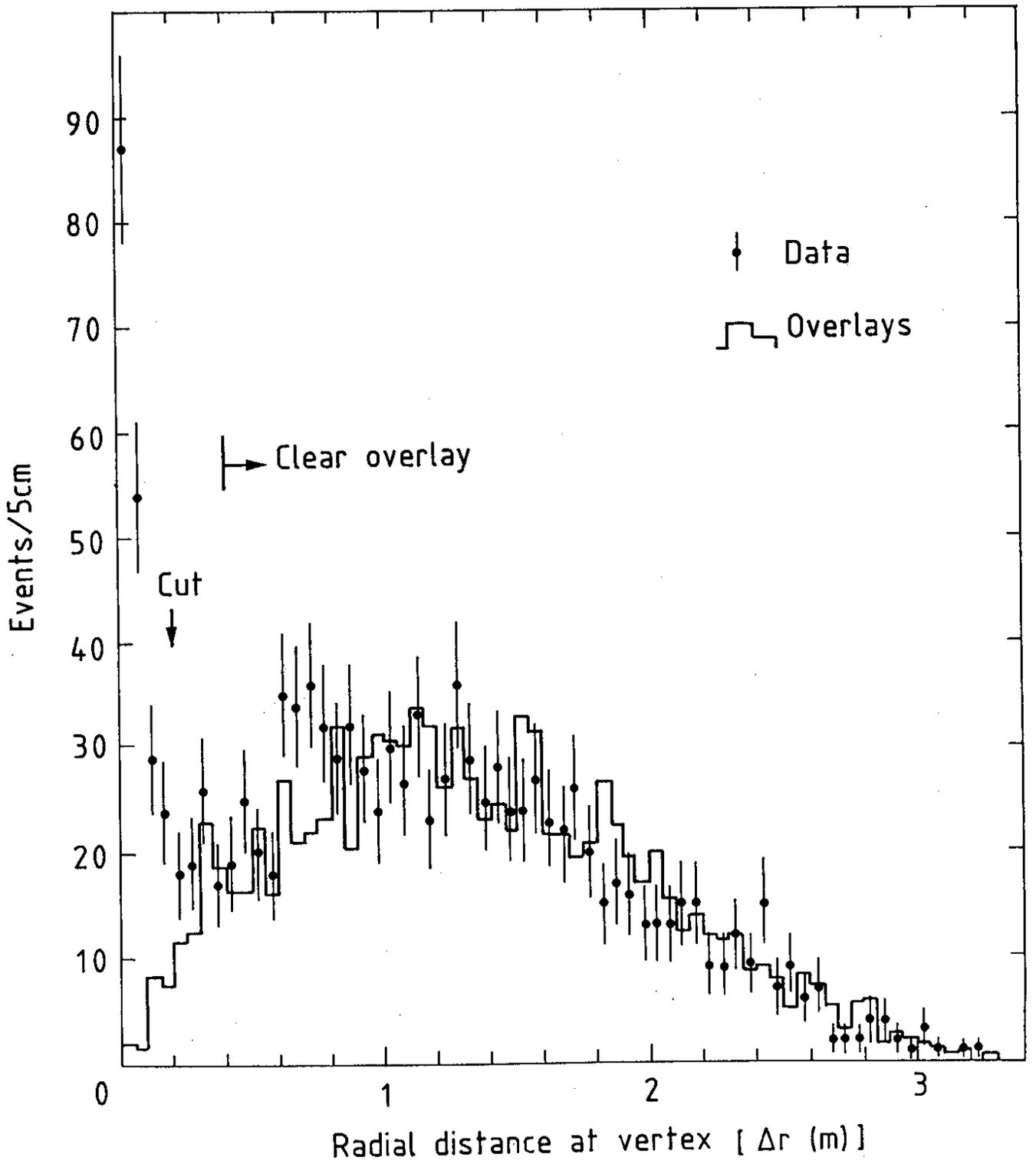
Data
Overlays
Clear overlay
Cut
Events/5cm
Radial distance at vertex [Δr (m)]
0
1
2
3
10
20
30
40
50
60
70
80
90

Fig. 4

prompt signal
overlay background
trimuon background
π and K decay background
a) ν
b) ν̄
$P_\mu > 6$
$P_\mu > 9$
$P_\mu > 15$
30 < E_{vis} < 100 GeV
100 < E_{vis} < 200 GeV
200 < E_{vis} < 300 GeV
150
100
50
Number of events

Fig. 5

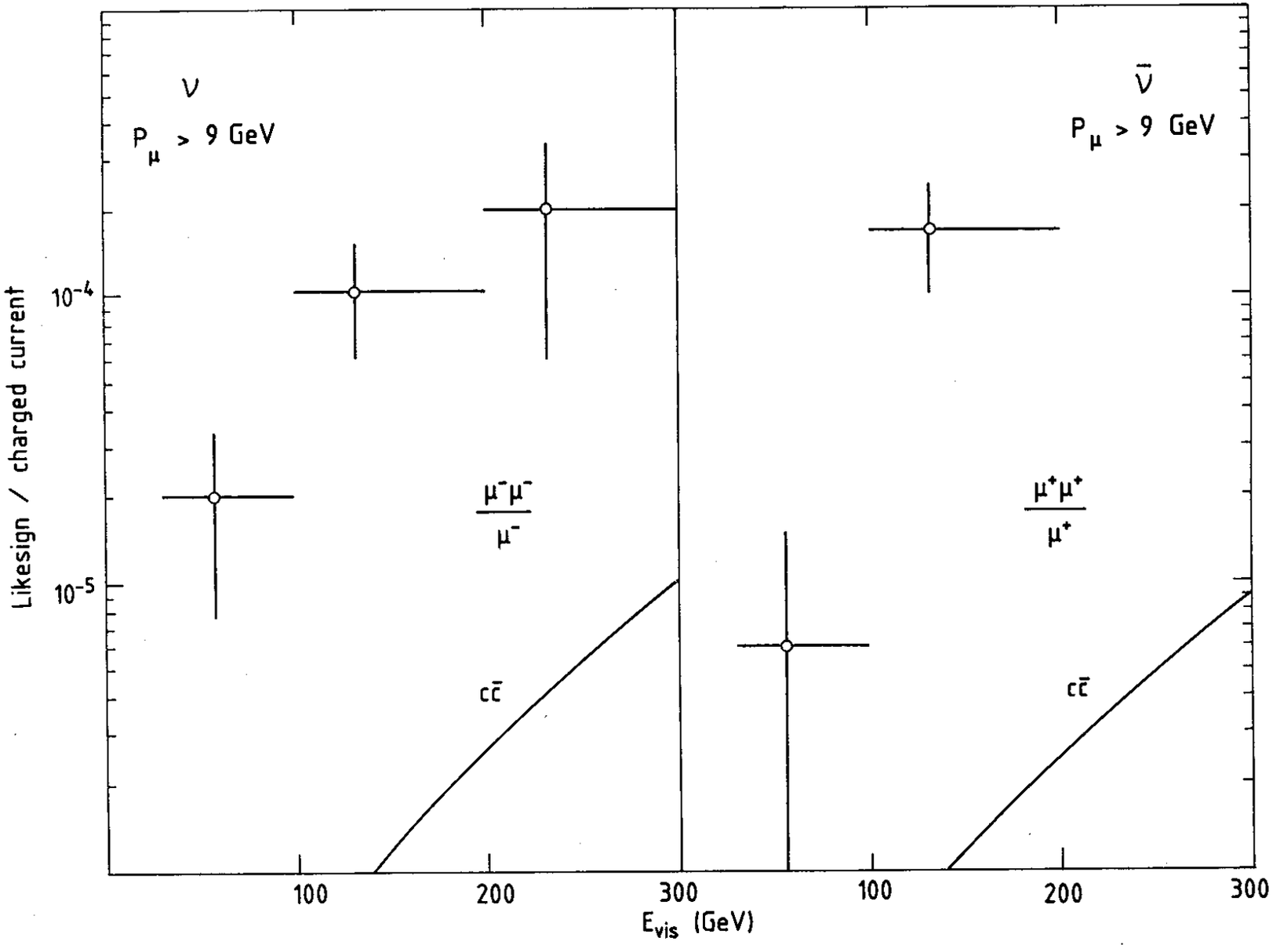
ν
P_μ > 9 GeV
ν̄
P_μ > 9 GeV
Likesign / charged current
10^-4
10^-5
μ⁻μ⁻ / μ⁻
μ⁺μ⁺ / μ⁺
cc̄
cc̄
100
200
300
100
200
300
E_vis (GeV)

Fig. 6

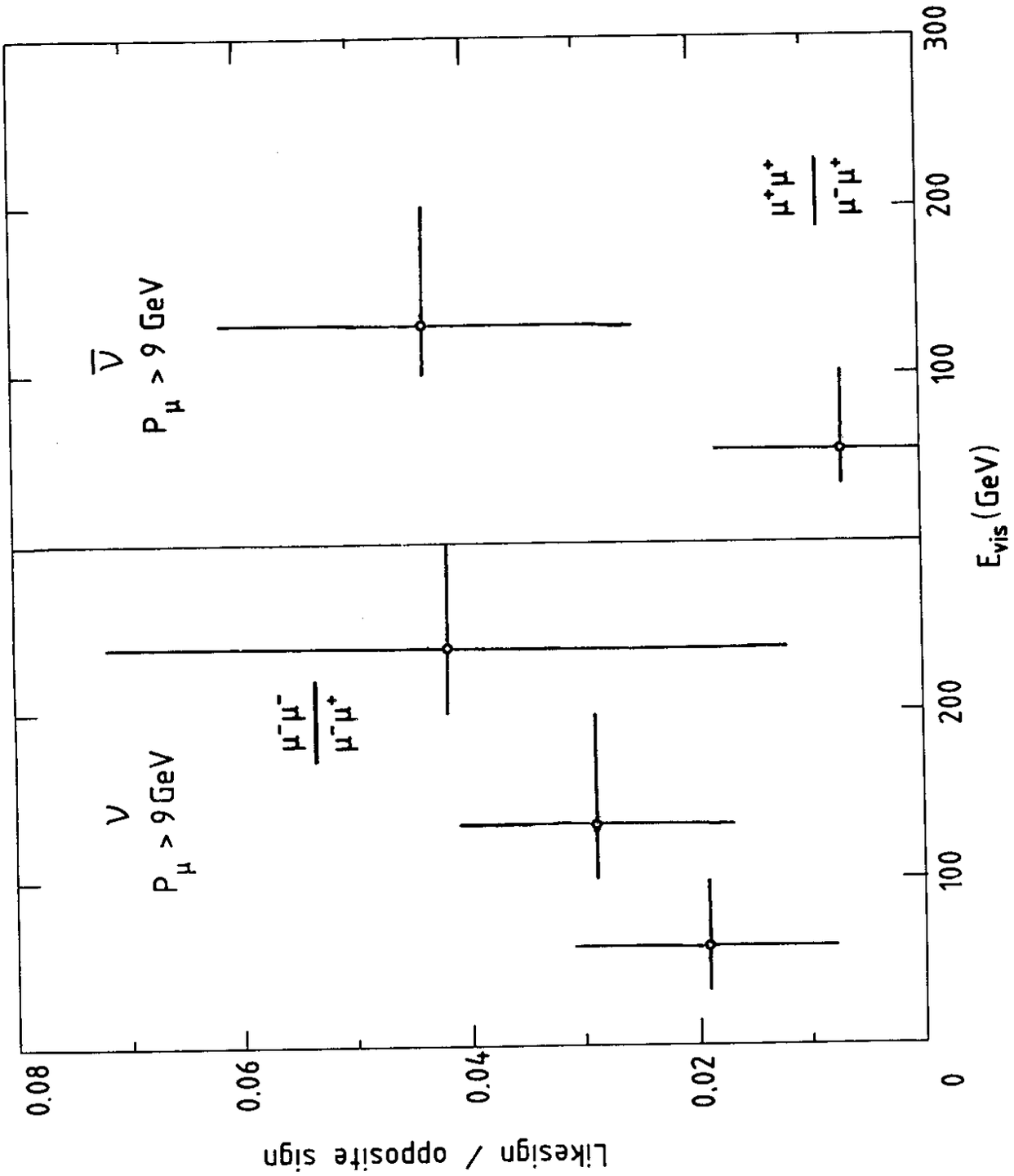
Likesign / opposite sign
0.08
0.06
0.04
0.02
0
100
200
300
E_{vis} (GeV)
ν
$P_\mu > 9$ GeV
$\frac{\mu^-\mu^-}{\mu^-\mu^+}$
$\bar{\nu}$
$P_\mu > 9$ GeV
$\frac{\mu^+\mu^+}{\mu^-\mu^+}$

Fig. 7

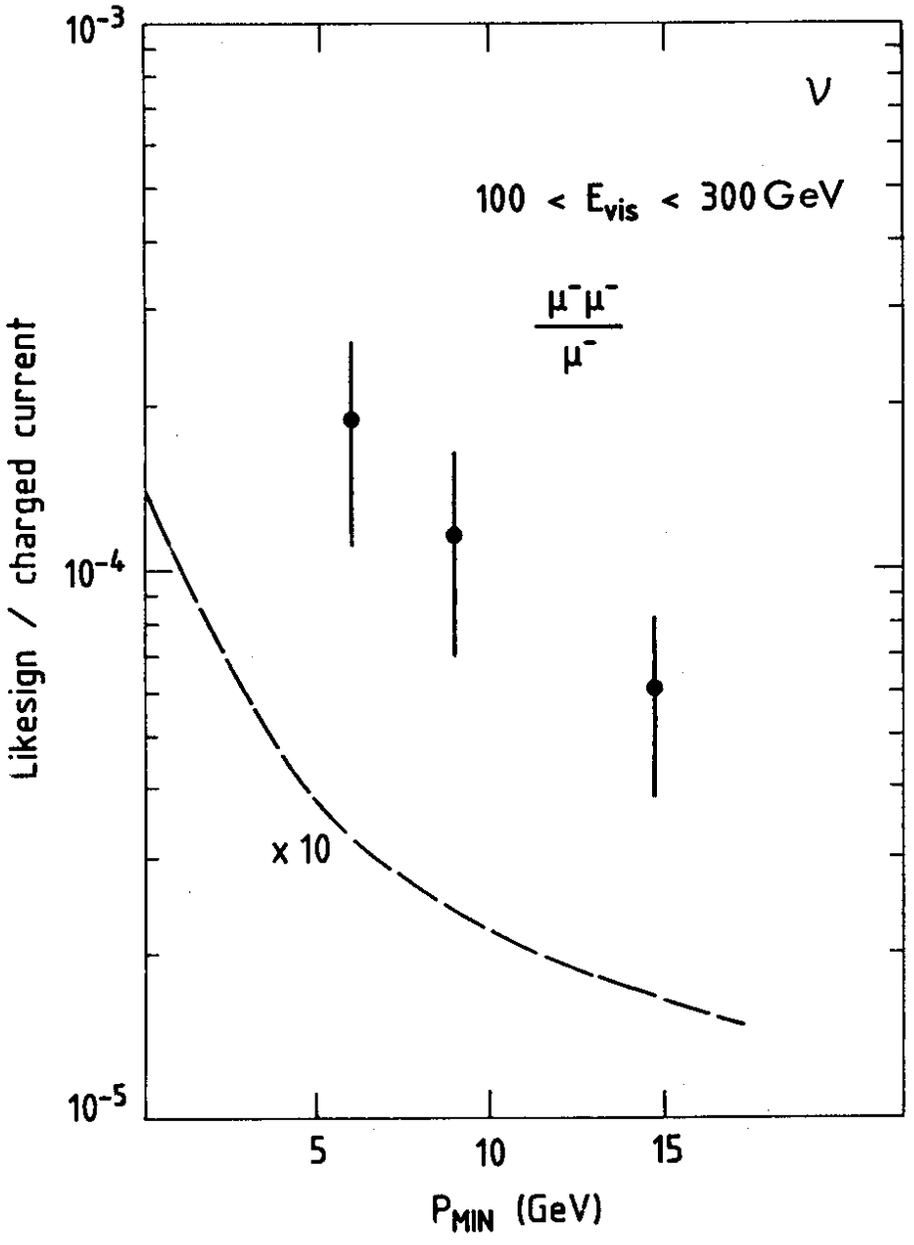
10^{-3}
10^{-4}
10^{-5}
Likesign / charged current
ν
$100 < E_{vis} < 300\,GeV$
$\frac{\mu^-\mu^-}{\mu^-}$
x 10
5
10
15
P_{MIN} (GeV)

Fig. 8

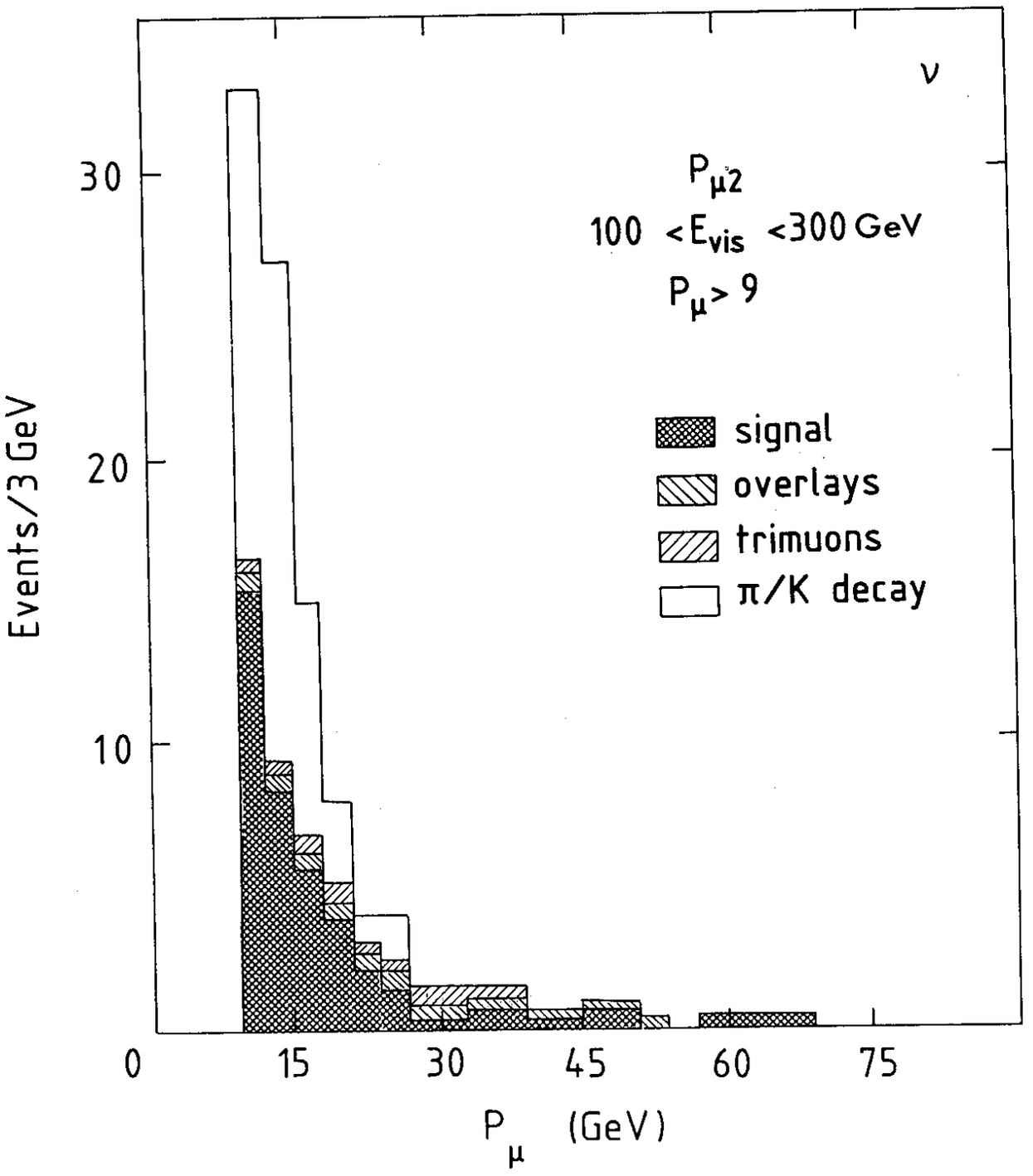
ν
$P_{\mu 2}$
100 < E_{vis} < 300 GeV
P_μ > 9
signal
overlays
trimuons
π/K decay
Events/3 GeV
30
20
10
0
15
30
45
60
75
P_μ (GeV)

Fig. 9

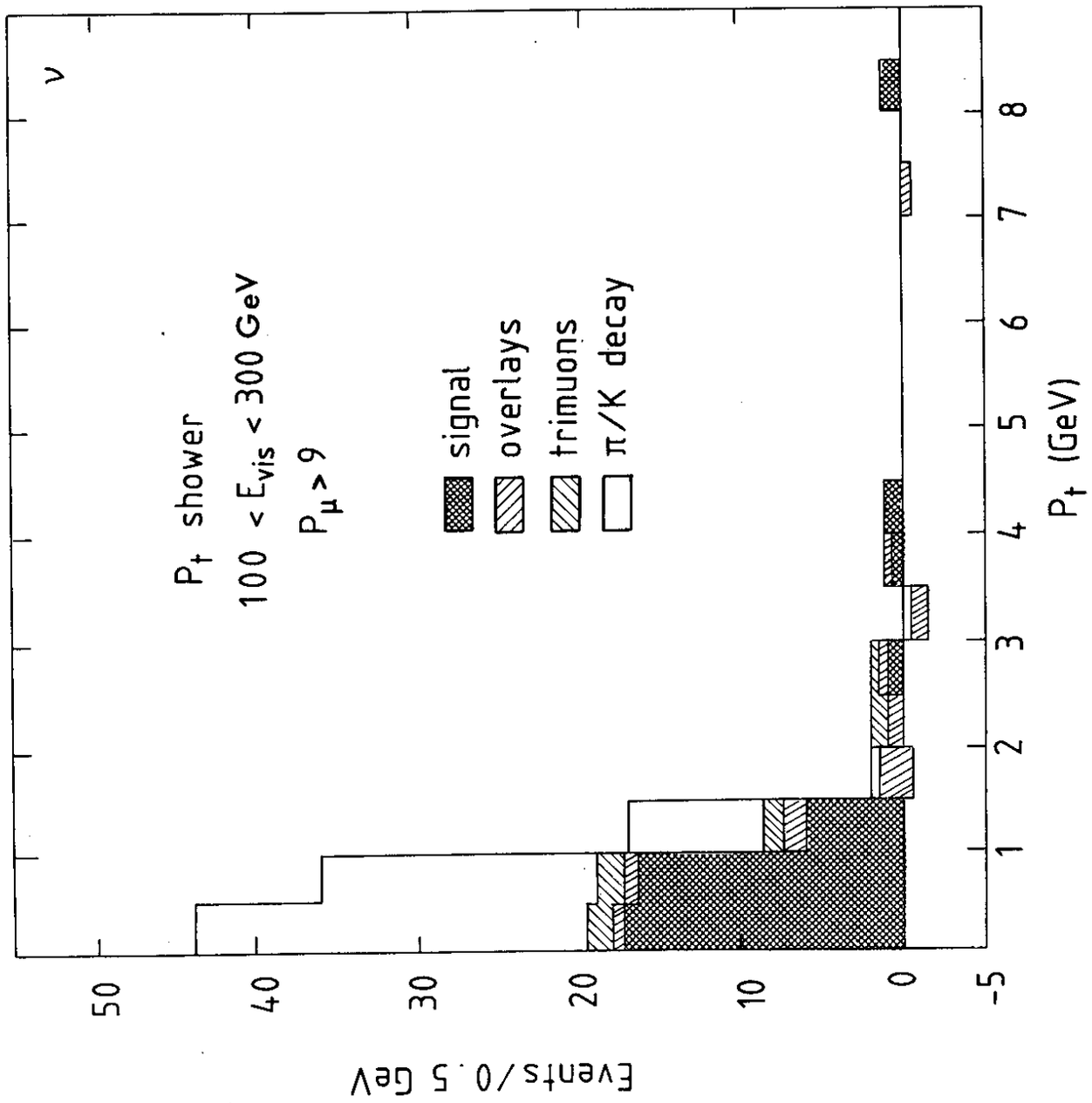
ν
P_t shower
$100 < E_{vis} < 300$ GeV
$P_\mu > 9$
signal
overlays
trimuons
π/K decay
Events/0.5 GeV
P_t (GeV)
50
40
30
20
10
0
-5
1
2
3
4
5
6
7
8

Fig. 10

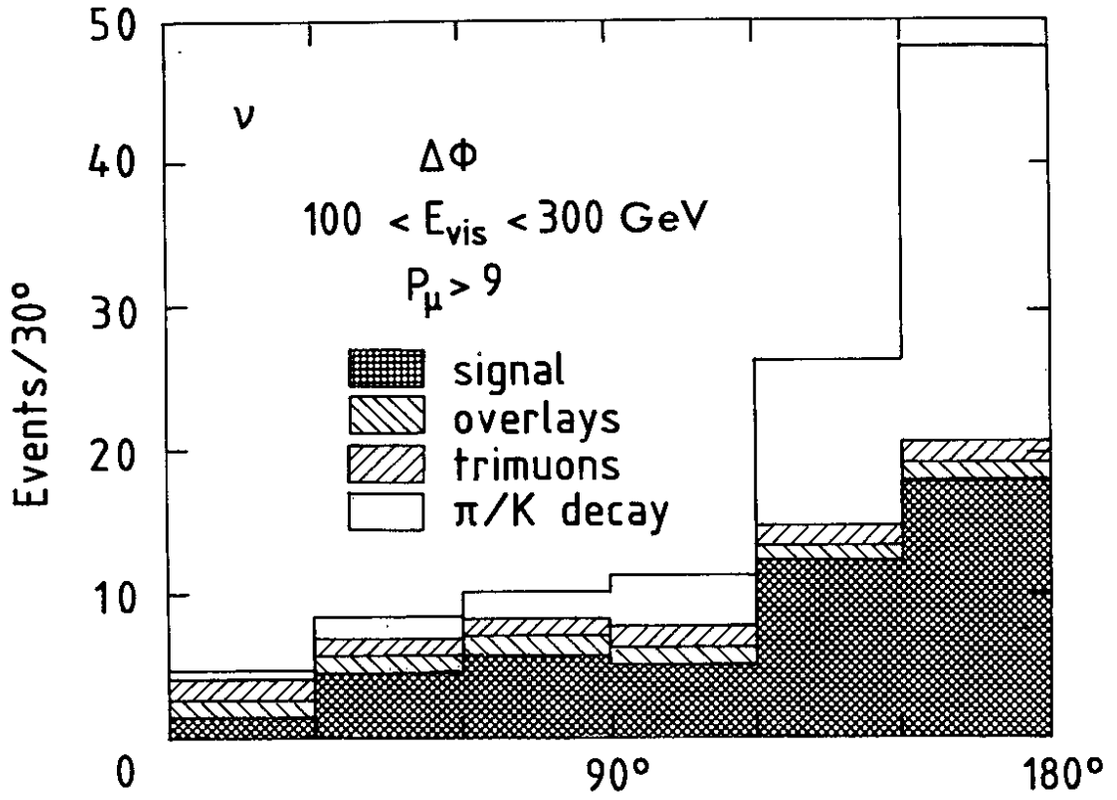
50
40
30
20
10
0
Events/30°
ν
ΔΦ
100 < E_vis < 300 GeV
P_μ > 9
signal
overlays
trimuons
π/K decay
90°
180°

Fig. 11

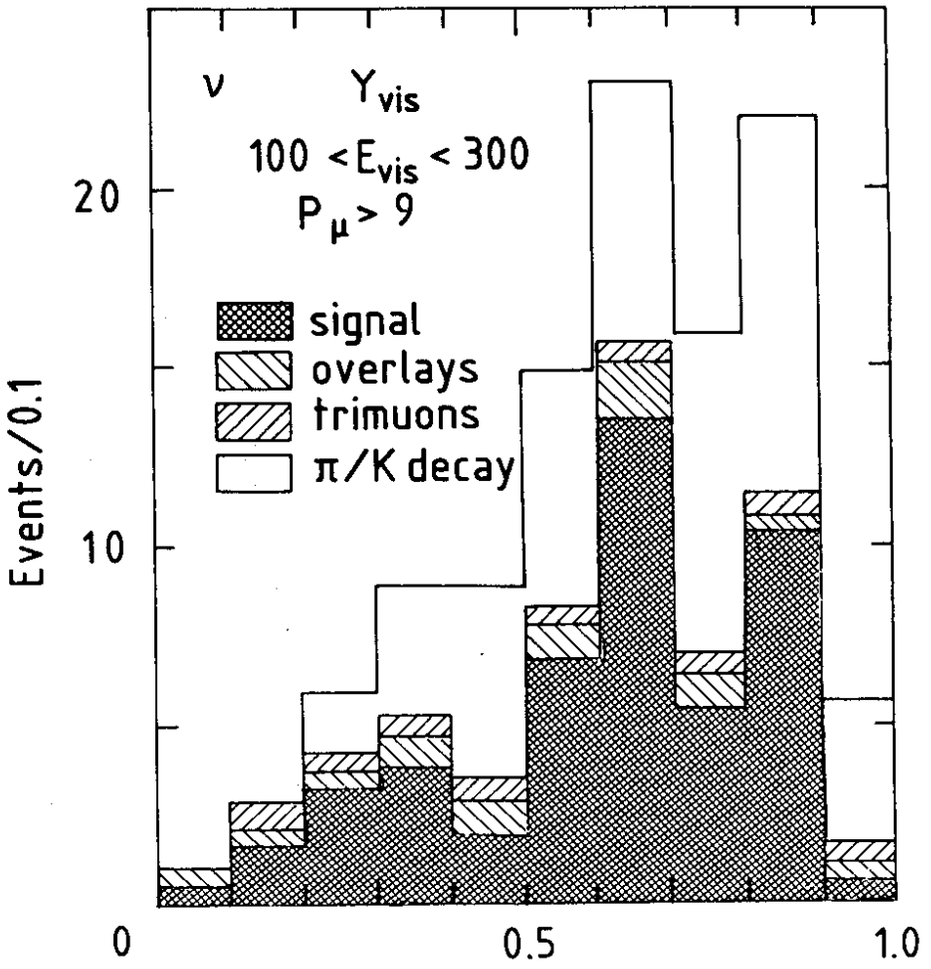
20
10
0
Events/0.1
ν
Y_vis
100 < E_vis < 300
P_μ > 9
signal
overlays
trimuons
π/K decay
0.5
1.0

Fig. 12

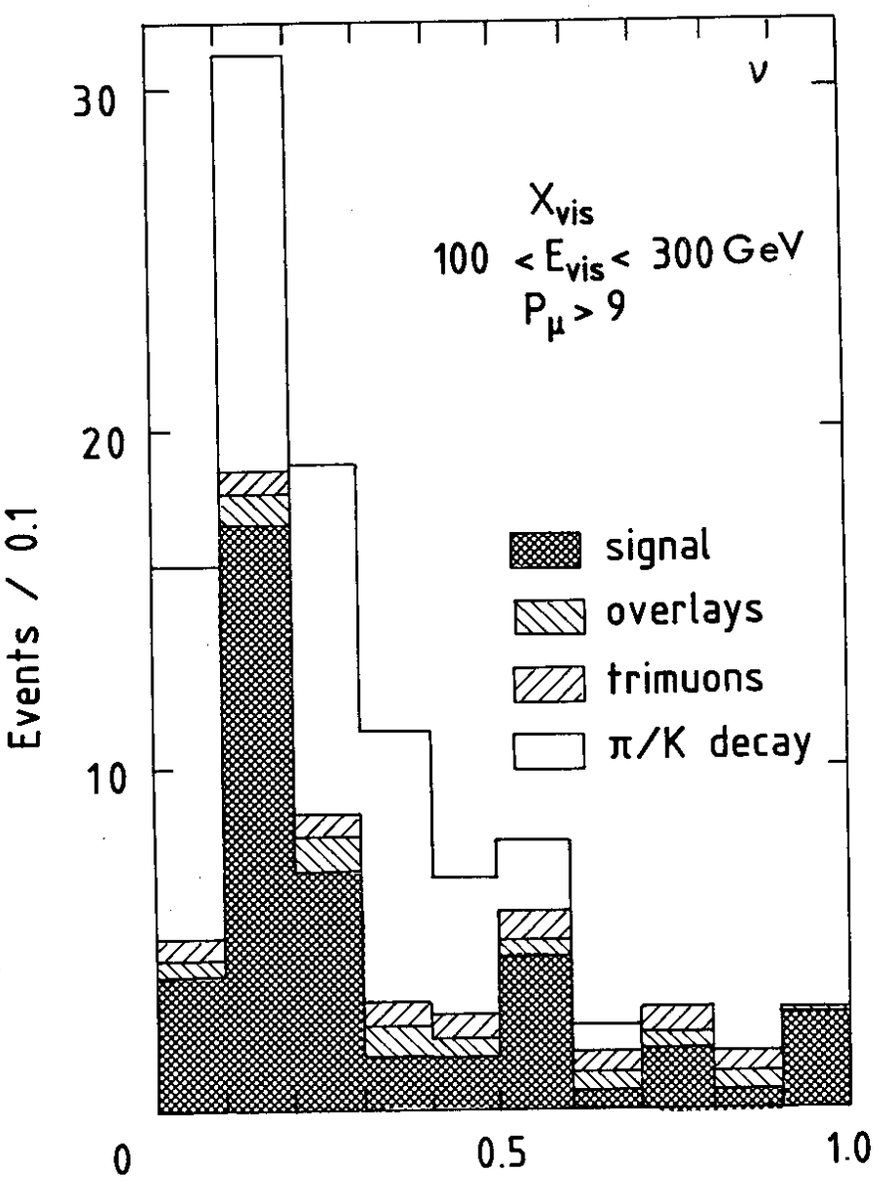
ν
X_{vis}
$100 < E_{vis} < 300$ GeV
$P_\mu > 9$
signal
overlays
trimuons
π/K decay
Events / 0.1
30
20
10
0
0.5
1.0

Fig. 13

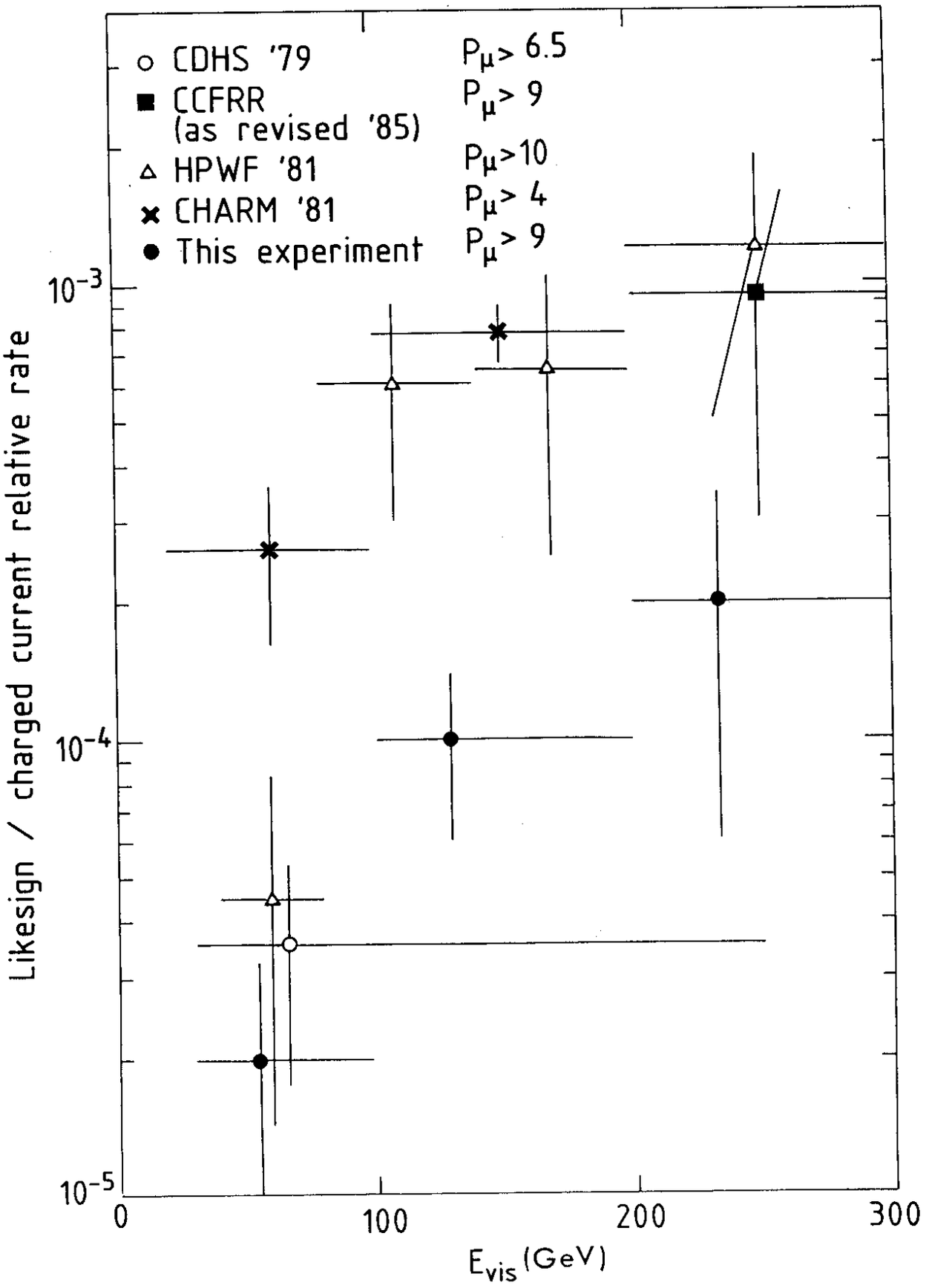
CDHS '79
CCFRR (as revised '85)
HPWF '81
CHARM '81
This experiment
$P_\mu > 6.5$
$P_\mu > 9$
$P_\mu > 10$
$P_\mu > 4$
$P_\mu > 9$
Likesign / charged current relative rate
10^{-3}
10^{-4}
10^{-5}
0
100
200
300
E_{vis} (GeV)

Fig. 14